Jets and elliptic flow correlations at low and high transverse momenta in ultrarelativistic $A + A$ collisions

L. V. Bravina*
Department of Physics, University of Oslo, PB 1048 Blindern, N-0316 Oslo, Norway

G. Kh. Eyyubova, V. L. Korotkikh, I. P. Lokhtin, S. V. Petrushanko, A. M. Snigirev,† and E. E. Zabrodin‡
Skobeltsyn Institute of Nuclear Physics, Lomonosov Moscow State University, RU-119991 Moscow, Russia

(Received 10 December 2020; revised 7 February 2021; accepted 3 March 2021; published 15 March 2021)

Data from the Large Hadron Collider on elliptic flow correlations at low and high p_T from Pb+Pb collisions at $\sqrt{s_{NN}} = 5.02$ TeV are analyzed and interpreted in the framework of the HYDJET++ model. This model allows us to describe simultaneously the region of both low and high transverse momenta and, therefore, to reproduce the experimentally observed nontrivial centrality dependence of elliptic flow correlations. The origin of the correlations between low and high-p_T flow components in peripheral lead-lead collisions is traced to correlations of particles in jets.

DOI: 10.1103/PhysRevC.103.034905

I. INTRODUCTION

A number of exquisite and intriguing phenomena, which have never been systematically studied at the accelerators of the previous generation, have been observed since the start of the Relativistic Heavy Ion Collider (RHIC) and Large Hadron Collider (LHC) heavy-ion programs. Azimuthal anisotropy of multiparticle production is among them as a powerful probe of collective properties of a new state of matter, quark-gluon plasma (QGP); see, e.g., [1]. It is commonly described by the Fourier decomposition of the invariant cross section in the form [2,3]

$$E\frac{d^3N}{dp^3} = \frac{d^2N}{2\pi p_T dp_T d\eta} \times \left\{1 + 2\sum_{n=1}^{\infty} v_n(p_T,\eta)\cos\left[n\left(\varphi - \Psi_n^{PP}\right)\right]\right\}, \quad (1)$$

where p_T is the transverse momentum, η is the pseudorapidity, φ is the azimuthal angle with respect to the participant plane Ψ_n^{PP} of nth order, and v_n are the Fourier coefficients:

$$v_n = \langle\langle\cos\left[n\left(\varphi - \Psi_n^{PP}\right)\right]\rangle\rangle. \quad (2)$$

The averaging in the last equation is performed over all particles in a single event and over all events.

The second harmonic, v_2, typically referred to as elliptic flow, is the most thoroughly investigated one (for review see [4] and references therein), because the eccentricity is the most pronounced coefficient in the initial conditions. It directly relates the anisotropic shape of the overlap region of the colliding nuclei to the corresponding anisotropy of the outgoing momentum distribution. At relatively low transverse momenta, $p_T < 3$–4 GeV/c, the azimuthal anisotropy results from a pressure-driven anisotropic expansion of the created matter, with more particles emitted in the direction of the largest pressure gradients [5]. At higher transverse momenta, this anisotropy is understood to arise from the path-length-dependent energy loss of partonic jets as they traverse the matter, with more jet particles emitted in the direction of shortest path length [6]. The correlations between soft and hard contributions to anisotropic flow have attracted a lot of attention; see, e.g., [7–9] and references therein. Considering initial-state collision geometry asymmetries and fluctuations, in Ref. [9] the authors were able to reproduce simultaneously the measurements of nuclear modification factor R_{AA} and elliptic flow v_2, that was a serious problem for most quenching models.

Recently, interesting correlations between v_2 values at high and low transverse momenta for different centralities were reported by the CMS Collaboration [10]. These correlations can also be seen in the ATLAS data [11]. In the present paper we analyze and interpret this intriguing experimental observation within the HYDJET++ model, which allows us to perform such analysis due to its remarkable feature, namely the presence of soft and hard physics simultaneously.

The paper is organized as follows. Basic features of the model are sketched in Sec. II. Here the origin of elliptic flow in the model, and interplay between the soft and hard physics, are discussed. Section III presents the results of model calculations of hadronic elliptic flow in Pb+Pb collisions at $\sqrt{s_{NN}} = 5.02$ TeV. The calculations are in fair agreement with

*Also at Skobeltsyn Institute of Nuclear Physics, Lomonosov Moscow State University, RU-119991 Moscow, Russia.

†Also at Bogoliubov Laboratory of Theoretical Physics, Joint Institute for Nuclear Research, RU-141980 Dubna, Russia.

‡Also at Department of Physics, University of Oslo, PB 1048 Blindern, N-0316 Oslo, Norway.

the experimental data, and the role of jets is clarified. Finally, conclusions are drawn in Sec. IV.

II. HYDJET++ MODEL

The model HYDJET++ [12] is a widely used event generator, which describes successfully the large number of physical observables measured in heavy-ion collisions during RHIC and LHC operation. Among them are centrality and pseudorapidity dependence of inclusive charged particle multiplicity, transverse momentum spectra, and $\pi^{\pm}\pi^{\pm}$ correlation radii in central Pb+Pb collisions [13], momentum and centrality dependence of elliptic and higher-order harmonic coefficients [14–18], flow fluctuations [19], angular dihadron correlations [20], forward-backward multiplicity correlations [21], jet quenching effects [22,23], and heavy meson production [24–26]. Details of the model can be found in the HYDJET++ manual [12].

The event generator includes two independent components: the soft, hydro-type state and the hard state resulting from in-medium multiparton fragmentation. The soft component is the thermal hadronic state generated on the chemical and thermal freeze-out hypersurfaces prescribed by the parametrization of relativistic hydrodynamics with preset freeze-out conditions. It represents the adapted version of the event generator FASTMC [27,28]. Particle multiplicities are calculated using the effective thermal volume approach and Poisson multiplicity distribution around its mean value, which is supposed to be proportional to the number of participating nucleons for a given impact parameter in an $A + A$ collision.

To simulate the elliptic flow effect, the hydro-inspired parametrization for the momentum and spatial anisotropy of soft hadron emission source is implemented [12,29]. Note that there are two parameters which govern the strength and the direction of the elliptic flow in the original HYDJET++ version [12]. The first one is the spatial anisotropy $\epsilon(b)$. It is responsible for the elliptic modulation of the final freeze-out hypersurface at a given impact parameter b. The second one is the momentum anisotropy $\delta(b)$, dealing with the modulation of the flow velocity profile. One can treat these two parameters as independent ones and, therefore, adjust them separately for each centrality by comparing to data. Although it provides better agreement with the data, this procedure leads to significant increase of the parameters to be tuned. Therefore, for the sake of simplicity we opted for another scenario, which is implemented in the basic version of the model. According to it, both parameters are correlated through the dependence of the elliptic flow coefficient v_2 on both $\epsilon(b)$ and $\delta(b)$, obtained in the hydrodynamic approach [29]:

$$v_2(\epsilon, \delta) \propto \frac{2(\delta - \epsilon)}{(1 - \delta^2)(1 - \epsilon^2)}. \tag{3}$$

Because $v_2(b)$ is proportional to the initial ellipticity $\epsilon_0(b) = b/2R_A$, where R_A is the radius of colliding nucleus, the relation between $\epsilon(b)$ and $\delta(b)$ reads [12]

$$\delta = \frac{\sqrt{1 + 4B(\epsilon + B)} - 1}{2B}, \quad B = C(1 - \epsilon^2)\epsilon, \quad \epsilon = k\epsilon_0. \tag{4}$$

Two new parameters C and k, entering the last expression, are independent of centrality and transverse momentum and, therefore, should be obtained from the fit to the experimental data.

In the hard sector the model propagates the hard partons through the expanding quark-gluon plasma and takes into account both collisional loss and gluon radiation due to parton rescattering. It is based on the PYQUEN partonic energy loss model [30]. The number of jets is generated according to a binomial distribution. Their mean number in an $A + A$ event is calculated as a product of the number of binary nucleon-nucleon (NN) subcollisions at a given impact parameter and the integral cross section of the hard process in NN collisions with the minimum transverse momentum transfer $p_T^{\min}$. The latter is the input parameter of the model. In the HYDJET++ framework, partons produced in (semi)hard processes with momentum transfer lower than $p_T^{\min}$ are considered as being "thermalized," and their hadronization products are automatically included in the soft component of the event.

Recall that there are many competing event generators successfully describing the soft [31–38] and hard [39–41] momentum components of particle production in heavy-ion collisions separately. The HYDJET++ is among the few ones [42,43] which allow us to study the soft and hard physics simultaneously.

III. RESULTS

To measure azimuthal correlations and to extract the Fourier coefficients, the CMS Collaboration employs the cumulant and the scalar product (SP) methods. The two- and fur-particle correlations are defined as

$$\langle\langle 2\rangle\rangle = \langle\langle e^{in(\varphi_1 - \varphi_2)}\rangle\rangle, \quad \langle\langle 4\rangle\rangle = \langle\langle e^{in(\varphi_1 + \varphi_2 - \varphi_3 - \varphi_4)}\rangle\rangle. \tag{5}$$

Here the double averaging is performed over all particle combinations and over all events. The multiparticle cumulant method is applied to measure v_2 from four-particle correlations. The second-order and fourth-order cumulants, $c_n\{2\}$ and $c_n\{4\}$, respectively, are given as [44]

$$c_n\{2\} = \langle\langle 2\rangle\rangle, \quad c_n\{4\} = \langle\langle 4\rangle\rangle - 2 \times \langle\langle 2\rangle\rangle^2. \tag{6}$$

For differential flow calculations the restricted two- and four-particle correlations, $\langle\langle 2'\rangle\rangle$ and $\langle\langle 4'\rangle\rangle$, are defined, where transverse momentum of one of the particles is limited to being within a certain p_T bin. The differential cumulants read

$$d_n\{2\} = \langle\langle 2'\rangle\rangle, \quad d_n\{4\} = \langle\langle 4'\rangle\rangle - 2 \times \langle\langle 2'\rangle\rangle \times \langle\langle 2\rangle\rangle. \tag{7}$$

Finally, the differential coefficients $v_n\{2\}(p_T)$ and $v_n\{4\}(p_T)$ are derived as

$$v_n\{2\}(p_T) = d_n\{2\} \times (c_n\{2\})^{-1/2}, \tag{8}$$

$$v_n\{4\}(p_T) = -d_n\{4\} \times (-c_n\{4\})^{-3/4}. \tag{9}$$

All the two- and four-particle correlations are calculated based on the Q-cumulant method [45], whereas the generic framework technique [46] was used by the CMS Collaboration in [10]. This approach, however, is equivalent to the Q-cumulant method we are using in this paper, as HYDJET++ simulation generates a uniform ϕ distribution. The same technique

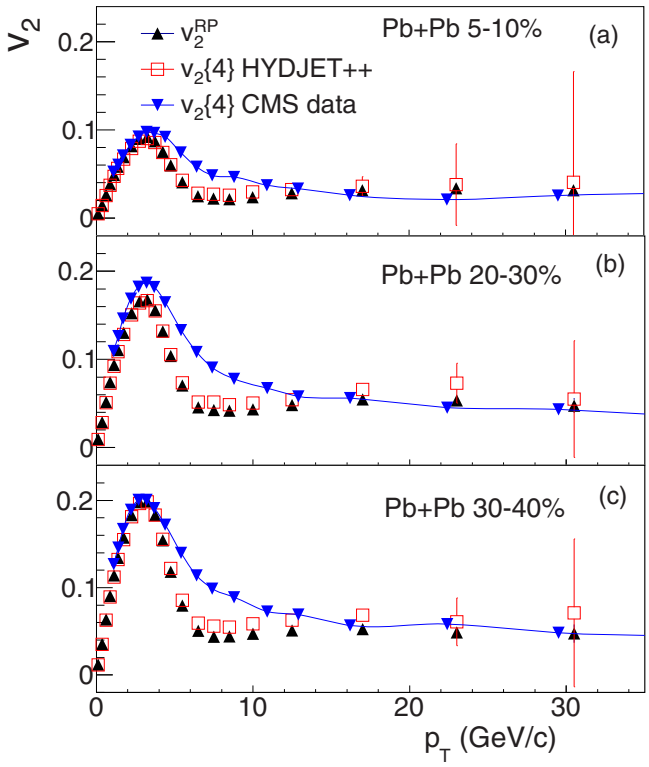

FIG. 1. The comparison of CMS data for $v_2\{4\}(p_T)$ [10] (triangles) and HYDJET++ calculations for $v_2\{4\}(p_T)$ (squares) and $v_2^{RP}(p_T)$ (circles) in Pb+Pb collisions at $\sqrt{s_{NN}} = 5.02$ TeV for the centralities (a) 5–10%, (b) 20–30%, and (c) 30–40%. Lines are drawn to guide the eye.

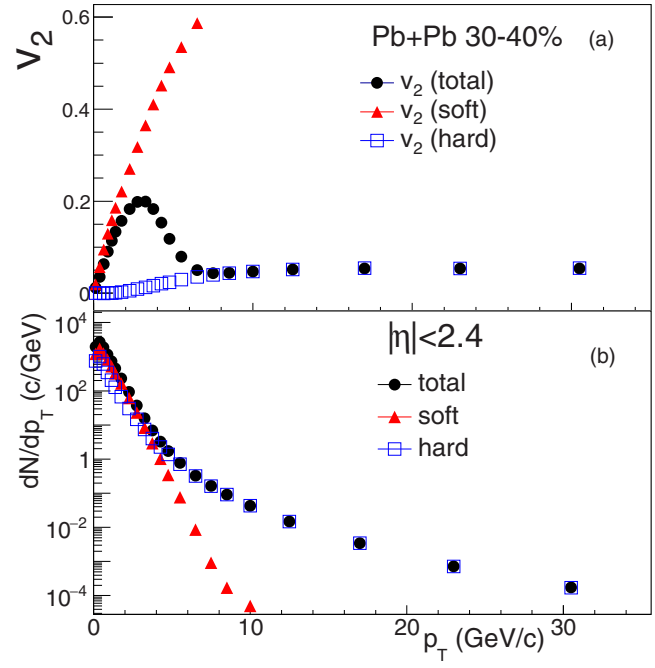

FIG. 2. (a) The soft (triangles) and hard (squares) components of the elliptic flow and resulting total flow $v_2^{RP}(p_T)$ (circles) within the pseudorapidity interval $|\eta| < 2.4$ in HYDJET++ for Pb+Pb collisions at $\sqrt{s_{NN}} = 5.02$ TeV with the centrality 30–40%. (b) The same as (a) but for the transverse momentum spectra dN/dp_T of hadrons.

is applied also to calculate the corresponding differential $v_2\{4\}(p_T)$ coefficients in the HYDJET++ model.

To compare model calculations with the data we generated Pb+Pb collisions at $\sqrt{s_{NN}} = 5.02$ TeV in seven centrality bins: $\sigma/\sigma_{\text{geo}} = 5$–$10\%$, 10–15% , 15–20% , 20–30%, 30–40%, 40–50%, and 50–60%. Statistics of generated events varies from 2×10^6 for semicentral to 7×10^6 for very peripheral collisions. Figure 1 shows the elliptic flow restored by the four-cumulant method from the HYDJET++ calculated events in comparison with the CMS data [10] for the centralities 5–10%, 20–30%, and 30–40%. The model-generated "true" value of the elliptic flow coefficient $v_2^{RP}(p_T)$ is also presented. It is calculated with respect to the reaction plane (RP), which is exactly known and is directed along the impact parameter **b** in the model. At relatively low transverse momenta, $p_T < 3$–4 GeV/c, the measured elliptic flow, $v_2\{4\}(p_T)$ (CMS), and the restored one, $v_2\{4\}(p_T)$ (HYDJET++), are practically equal to the generated original elliptic coefficient $v_2^{RP}(p_T)$. It is not surprising, because in this momentum region the underlying v_2 distributions are close to Gaussian type and the bulk of produced particles are mainly correlated with the reaction plane only and nonflow correlations are relatively small. One would expect to see a deviation of $v_2\{4\}$ from v_2^{RP} in the most central and peripheral collisions. This problem lies out of scope of our present study. This was partly discussed in our previous work; see [16]. At higher transverse momenta, $p_T > 10$ GeV/c, which is the region of the special interest here, the values of the measured elliptic flow and the flow restored from the model calculations are close to each other, but noticeably larger than the generated elliptic flow $v_2^{RP}(p_T)$. In the intermediate region, $4 < p_T < 10$ GeV/c, both model calculated coefficients, $v_2^{RP}(p_T)$ and $v_2\{4\}(p_T)$ (HYDJET++), lie below the CMS data for all three centrality bins. This circumstance, however, is unimportant here, since our study is limited to the intervals $p_T \leqslant 1.25$ GeV/c and $p_T \geqslant 14$ GeV/c, in which the agreement between the results of model calculations and experimental data is very good.

Figure 2(a) illustrates the structure of elliptic flow in HYDJET++. Here the coefficients $v_2^{RP}(p_T)$ are calculated with respect to the reaction plane separately for each component, soft and hard, together with the resulting total value. This illustration shows the slight model drawback in the intermediate momentum region. Originally, the model includes the adequate description of soft and hard physics. In the intermediate p_T region the result is obtained by a simple superposition of two independent contributions. Note that the combined dN/dp_T spectrum of particles at $p_T \geqslant 5$ GeV/c is dominated by hadrons from the hard subprocesses, as displayed in Fig. 2(b). The crosslinking is regulated by one parameter, $p_T^{\min}$, which is the minimum transverse momentum transfer in a hard parton subprocess. For the transverse momentum spectra this procedure is painless since the crosslinking takes place for a continuous function, and its fracture is smoothed out by the overlapping of particles from both contributions. As a result, we describe effectively the transverse momentum spectra even in the intermediate region also [13] without

any additional mechanism. For elliptic flow coefficients the crosslinking takes place for a "discontinuous" function; see the crosslinking region of $p_T \simeq 4$–8 GeV/c, where $v_2^{RP}(p_T)$ (soft) and $v_2^{RP}(p_T)$ (hard) have the quite different values. Thus, the simple smoothing is not enough to describe this region by a simple superposition. It means that some improvements of the model are required to describe successfully the whole p_T region. For instance, it can be a minijet production or some other mechanism. Fortunately, this "problematic" region of the model is not used in the present flow correlation analysis.

Now we focus on the high transverse momentum region, for which, to study with good accuracy, a large number of events should be generated. In this region the HYDJET++ flow, restored by the cumulant method, is close to the measured one, but it is visibly larger than the elliptic flow in the reaction plane generated in the model. This observation requires an explanation. The azimuthal anisotropy arises in the model as a result of jet quenching; see [22,23]. Due to the path-length-dependent energy loss of partonic jets as they traverse the matter, the jet particles become correlated with the reaction plane. However, the particle correlations relative to the jet axis remain also. Unlike the region of low transverse momentum, there are at least two singled out directions, the reaction plane and the jet axis, relative to which particles are correlated. In this case we can decompose the azimuthal distribution in the form

$$\frac{dN}{d\varphi} = N_0\big(1 + 2v_2^{RP}\cos\big[2\big(\varphi - \Psi_2^{RP}\big)\big] + 2v_2^{\rm jet}\cos\big[2\big(\varphi - \Psi_2^{\rm jet}\big)\big]\big), \tag{10}$$

where the direction of jet axis $\Psi_2^{\rm jet}$ is randomly oriented with respect to the reaction plane Ψ_2^{RP}, which is set to zero in the model calculations. N_0 is the normalization factor. The two- and four-particle correlations are estimated in a toy model (10) as

$$\langle\langle 2\rangle\rangle \simeq \big(v_2^{RP}\big)^2 + \big(v_2^{\rm jet}\big)^2, \quad \langle\langle 4\rangle\rangle \simeq \big[\big(v_2^{RP}\big)^2 + \big(v_2^{\rm jet}\big)^2\big]^2 \tag{11}$$

and they are sensitive to both types of correlations discussed above. Herewith $\langle\langle 2\rangle\rangle^{1/2}$ and $\langle\langle 4\rangle\rangle^{1/4}$ are *always larger* than the "true" elliptic coefficient $v_2^{RP}(p_T)$ in which we are interested. Unfortunately, one cannot demonstrate this analytically for differential flow $v_2\{4\}(p_T)$ defined by Eq. (9). However, HYDJET++ calculations shown in Fig. 1 suggest that $v_2\{4\}(p_T)$ (HYDJET++) is systematically larger than $v_2^{RP}(p_T)$ at transverse momenta higher than 10 GeV/c for all centralities. In this interval of p_T only jets contribute to the spectrum dN/dp_T in our approach. Naturally, we try to understand whether strong particle correlations relative to the jet axis can lead to such an effect. The estimation (11) strongly supports this assumption.

The correlations between the low-p_T and high-p_T elliptic flow which are the main issue of our study are displayed in Fig. 3(a). The picked-up intervals are $14 < p_T < 20$ GeV/c for high and $1.0 < p_T < 1.25$ GeV/c for low transverse momenta. One can see that the model calculations, $v_2\{4\}(p_T)$ (HYDJET++), reproduce the experimentally observed centrality

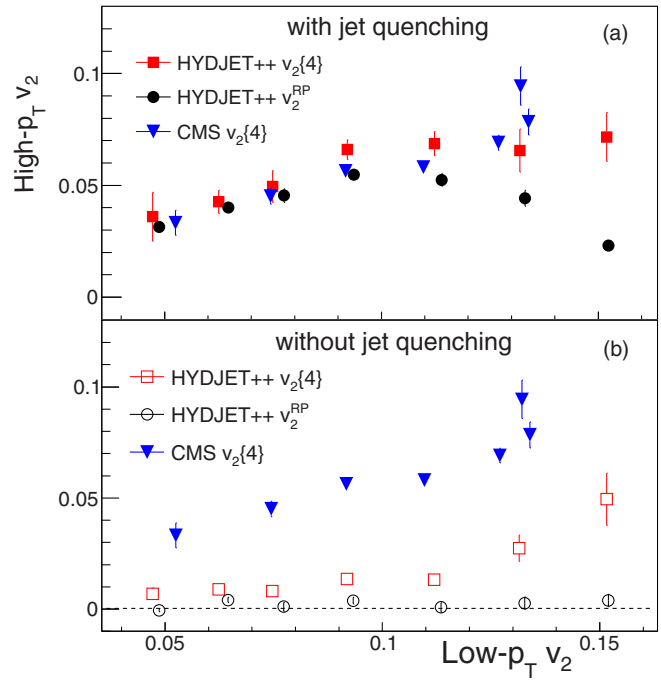

FIG. 3. The correlation between v_2 values at low and high p_T in Pb+Pb collisions at $\sqrt{s_{NN}} = 5.02$ TeV as a function of centrality. The points represent the centrality bins 5–10%, 10–15%, 15–20%, 20–30%, 30–40%, 40–50%, and 50–60%. The model results are presented for v_2^{RP} (circles) and $v_2\{4\}$ (squares). Data (triangles) are taken from [10]. Model calculations are performed (a) with and (b) without jet quenching. For better visualization, squares are shifted to the left compared to circles in the first five bins.

dependence of the flow correlations fairly well except in the last centrality bin, while the generated original elliptic flow $v_2^{RP}(p_T)$ at high p_T goes always lower than the restored flow in accordance with the explanation above. The deviations become significant for the centralities larger than 30–40%. In this centrality interval the anisotropy caused by the jet quenching begins to die out, but particles remain correlated with the axes of jets. Note that in the low-p_T region the integrated values of v_2 in the model are lower than the data. This is due to the simplification, discussed in Sec. II, aiming to reduce the number of free parameters in the model. To reach better quantitative agreement with the data one has to treat both anisotropy parameters, $\varepsilon(b)$ and $\delta(b)$, as independent ones; see [19]. This circumstance, however, does not affect the main results associated with identifying the role of jets in the behavior of cumulants. Note also that in the high-p_T sector the agreement between the model results and the data is good.

Figure 3(b) demonstrates the comparison of model calculations without jet quenching effects with the data. In this case $v_2^{RP} = 0$ at high p_T and the correlations relative to the jet axis contribute to the fourth-order cumulant only, but the magnitude of jet correlations is not strong enough to reproduce data. Thus, in the collisions with centrality up to 30–40% the azimuthal anisotropy due to jet quenching reveals itself, whereas in more peripheral collisions the jet correlations contribute significantly to the fourth-order cumulant. The reason

is as follows. Since in peripheral heavy-ion collisions there are simply quantitatively fewer nucleon-nucleon collisions, fewer jets are produced. In the limiting case there is one back-to-back pair, and the method sees this axis and anisotropy. In more central collisions there are many jet pairs. They are all distributed randomly in azimuth, therefore the anisotropy caused by jets tends to zero.

It is worth noting that jets were the main source of violation of the number-of-constituent-quark (NCQ) scaling in HYDJET++ calculations of differential elliptic [14,15] and triangular [18] flow. The linear fit [10], performed by the CMS Collaboration to data on elliptic flow correlations at low and high transverse momenta, also indicates some sort of scaling behavior. In contrast to situation with the NCQ scaling, here jets work toward the scaling fulfillment.

IV. CONCLUSIONS

The phenomenological analysis of elliptic flow correlations at low and high p_T in Pb+Pb collisions at center-of-mass energy 5.02 TeV per nucleon pair has been performed within the two-component HYDJET++ model. These correlations are stipulated by the fact that the magnitudes of anisotropy at low and high p_T are mainly determined by the value of initial ellipticity of the nuclei overlapping. At relatively low transverse momenta, $p_T < 3$–4 GeV$/c$, the model-generated elliptic flow $v_2^{RP}(p_T)$ and its value restored by the four-cumulant method, $v_2\{4\}(p_T)$ (HYDJET++), are very close to the differential elliptic flow $v_2\{4\}(p_T)$ measured by the CMS Collaboration. At high transverse momenta $p_T > 10$ GeV$/c$ the cumulants are sensitive to both the anisotropy due to jet quenching, v_2^{RP}, and the particle correlations with the jet axis, $v_2^{\rm jet}$. In the collisions with centrality up to 30–40% the four-cumulant method "measures" mainly the azimuthal anisotropy due to jet quenching, whereas in more peripheral collisions it is affected primarily by the particle correlations inside jets. The model calculations restored by this method, $v_2\{4\}(p_T)$ (HYDJET++), reproduce the experimentally observed centrality dependence of elliptic flow correlations rather well without any additional tuning of model parameters.

ACKNOWLEDGMENTS

Fruitful discussions with A. I. Demyanov and L. V. Malinina are gratefully acknowledged. This work was supported in parts by Russian Foundation for Basic Research (RFBR) under Grants No. 18-02-00155, No. 18-02-40084, and No. 18-02-40085. L.V.B. and E.E.Z. acknowledge support of the Norwegian Research Council (NFR) under Grant No. 255253/F50, "CERN Heavy Ion Theory."

[1] *Proceedings of Quark Matter 2018*, edited by F. Antinori, A. Dainese, P. Giubellini, V. Greco, M. P. Lombardi, and E. Scomparin [Nucl. Phys. A **982**, 1 (2019)].
[2] S. Voloshin and Y. Zhang, Z. Phys. C **70**, 665 (1996).
[3] A. M. Poskanzer and S. A. Voloshin, Phys. Rev. C **58**, 1671 (1998).
[4] U. Heinz and R. Snellings, Annu. Rev. Nucl. Part. Sci. **63**, 123 (2013).
[5] J. Y. Ollitrault, Phys. Rev. D **46**, 229 (1992); **48**, 1132 (1993).
[6] M. Gyulassy, I. Vitev, and X.-N. Wang, Phys. Rev. Lett. **86**, 2537 (2001).
[7] N. Armesto, C. A. Salgado, and U. A. Wiedemann, Phys. Rev. C **72**, 064910 (2005).
[8] J. Jia, Phys. Rev. C **87**, 061901(R) (2013).
[9] J. Noronha-Hostler, B. Betz, J. Noronha, and M. Gyulassy, Phys. Rev. Lett. **116**, 252301 (2016).
[10] A. M. Sirunyan *et al.* (CMS Collaboration), Phys. Lett. B **776**, 195 (2018).
[11] M. Aaboud *et al.* (ATLAS Collaboration), Eur. Phys. J. C **78**, 997 (2018).
[12] I. P. Lokhtin, L. V. Malinina, S. V. Petrushanko, A. M. Snigirev, I. Arsene, and K. Tywoniuk, Comput. Phys. Commun. **180**, 779 (2009).
[13] I. P. Lokhtin, A. V. Belyaev, L. V. Malinina, S. V. Petrushanko, E. P. Rogochaya, and A. M. Snigirev, Eur. Phys. J. C **72**, 2045 (2012).
[14] G. Eyyubova, L. V. Bravina, E. Zabrodin, V. L. Korotkikh, I. P. Lokhtin, L. V. Malinina, S. V. Petrushanko, and A. M. Snigirev, Phys. Rev. C **80**, 064907 (2009).
[15] L. Bravina, B. H. Brusheim Johansson, G. Eyyubova, and E. Zabrodin, Phys. Rev. C **87**, 034901 (2013).
[16] L. V. Bravina, B. H. Brusheim Johansson, G. Kh. Eyyubova, V. L. Korotkikh, I. P. Lokhtin, L. V. Malinina, S. V. Petrushanko, A. M. Snigirev, and E. E. Zabrodin, Eur. Phys. J. C **74**, 2807 (2014).
[17] L. Bravina, B. H. Brusheim Johansson, E. E. Zabrodin, G. Eyyubova, V. L. Korotkikh, I. P. Lokhtin, L. V. Malinina, S. V. Petrushanko, and A. M. Snigirev, Phys. Rev. C **89**, 024909 (2014).
[18] J. Crkovskà *et al.*, Phys. Rev. C **95**, 014910 (2017).
[19] L. V. Bravina, E. S. Fotina, V. L. Korotkikh, I. P. Lokhtin, L. V. Malinina, E. N. Nazarova, S. V. Petrushanko, A. M. Snigirev, and E. E. Zabrodin, Eur. Phys. J. C **75**, 588 (2015).
[20] G. Eyyubova, V. L. Korotkikh, I. P. Lokhtin, S. V. Petrushanko, A. M. Snigirev, L. V. Bravina, and E. E. Zabrodin, Phys. Rev. C **91**, 064907 (2015).
[21] E. E. Zabrodin, I. P. Lokhtin, A. A. Sidorova, and A. S. Chernyshov, J. Exp. Theor. Phys. **130**, 660 (2020).
[22] I. P. Lokhtin, A. V. Belyaev, and A. M. Snigirev, Eur. Phys. J. C **71**, 1650 (2011).
[23] I. P. Lokhtin, A. A. Alkin, and A. M. Snigirev, Eur. Phys. J. C **75**, 452 (2015).
[24] I. P. Lokhtin, A. V. Belyaev, G. Ponimatkin, E. Yu. Pronina, and G. Kh. Eyyubova, J. Phys. G **43**, 125104 (2016).
[25] I. P. Lokhtin, A. V. Belyaev, G. Ponimatkin, E. Yu. Pronina, and G. Kh. Eyyubova, J. Exp. Theor. Phys. **124**, 244 (2017).
[26] I. P. Lokhtin and A. A. Sidorova, J. Exp. Theor. Phys. **128**, 586 (2019).
[27] N. S. Amelin, R. Lednicky, T. A. Pocheptsov, I. P. Lokhtin, L. V. Malinina, A. M. Snigirev, Iu. A. Karpenko, and Yu. M. Sinyukov, Phys. Rev. C **74**, 064901 (2006).

[28] N. S. Amelin, R. Lednicky, I. P. Lokhtin, L. V. Malinina, A. M. Snigirev, Iu. A. Karpenko, Yu. M. Sinyukov, I. Arsene, and L. Bravina, Phys. Rev. C **77**, 014903 (2008).
[29] U. A. Wiedemann, Phys. Rev. C **57**, 266 (1998).
[30] I. P. Lokhtin and A. M. Snigirev, Eur. Phys. J. C **45**, 211 (2006).
[31] S. Ryu, S. Jeon, C. Gale, B. Schenke, and C. Young, Nucl. Phys. A **904**, 389c (2013).
[32] S. A. Bass *et al.*, Prog. Part. Nucl. Phys. **41**, 255 (1998).
[33] M. Bleicher *et al.*, J. Phys. G **25**, 1859 (1999).
[34] E. E. Zabrodin, C. Fuchs, L. V. Bravina, and A. Faessler, Phys. Lett. B **508**, 184 (2001).
[35] J. Bleibel, L. V. Bravina, and E. E. Zabrodin, Phys. Rev. D **93**, 114012 (2016).
[36] Z.-W. Lin, C. M. Ko, B.-A. Li, B. Zhang, and S. Pal, Phys. Rev. C **72**, 064901 (2005).
[37] W. Cassing and E. L. Bratkovskaya, Phys. Rep. **308**, 65 (1999).
[38] A. Kisiel, T. Taluc, W. Broniowski, and W. Florkowski, Comput. Phys. Commun. **174**, 669 (2006).
[39] T. Sjostrand, S. Ask, J. R. Christiansen, R. Corke, N. Desai, P. Ilten, S. Mrenna, S. Prestel, C. O. Rasmussen, and P. Z. Skands, Comput. Phys. Commun. **191**, 159 (2015).
[40] R. K. Elayavalli and K. C. Zapp, J. High Energy Phys. 07 (2017) 141.
[41] J. Xu, J. Liao, and M. Gyulassy, J. High Energy Phys. 02 (2016) 169.
[42] T. Pierog, Iu. Karpenko, J. M. Katzy, E. Yatsenko, and K. Werner, Phys. Rev. C **92**, 034906 (2015).
[43] S. Ostapchenko, Phys. Rev. D **83**, 014018 (2011).
[44] N. Borghini, P. M. Dinh, and J.-Y. Ollitrault, Phys. Rev. C **64**, 054901 (2001).
[45] A. Bilandzic, R. Snellings, and S. Voloshin, Phys. Rev. C **83**, 044913 (2011).
[46] A. Bilandzic, C. H. Christensen, K. Gulbrandsen, A. Hansen, and Y. Zhou, Phys. Rev. C **89**, 064904 (2014).